ChemComm

COMMUNICATION

View Article Online
View Journal

Cite this: DOI: 10.1039/c8cc01674g

Received 28th February 2018,
Accepted 12th April 2018

DOI: 10.1039/c8cc01674g

rsc.li/chemcomm

High pressure NMR reveals conformational perturbations by disease-causing mutations in amyloid β-peptide†

David J. Rosenman,[a] Nicolina Clemente,[b] Muhammad Ali,[c] Angel E. García[abd] and Chunyu Wang *[ab]

Here we present the high pressure NMR characterization of Aβ42 and two Aβ40 variants with Alzheimer-causing mutations E22G and D23N. While chemical shifts only identified localized changes at ambient pressure compared with Aβ40, high pressure NMR revealed a common site with heightened pressure sensitivity at Q15, K16 and L17 in all three variants, which correlates to higher β-propensity at central hydrophobic cluster (CHC) and faster aggregation.

Amyloid β (Aβ) is implicated in the pathogenesis of Alzheimer's disease (AD), a neurodegenerative disease that affects about 47 million people worldwide.[1] Aβ aggregates to form senile plaques in the brain, a pathological hallmark of AD. Aβ is generated from amyloid precursor protein (APP) through sequential cleavage by β- and γ-secretase. Aβ40 and Aβ42, composed of 40 and 42 residues, respectively, are the most common species of Aβ in the human brain. Aβ42 aggregates much faster than Aβ40[2,3] through distinct mechanisms.[4] While Aβ monomers are relatively benign,[5] they aggregate into neurotoxic species, including fibrils,[6,7] protofibrils[8] and oligomers.[9] Aβ aggregates observed in AD brains are correlated to clinical manifestations of dementia.[10–12] Compared with Aβ40, Aβ42 is significantly more toxic to neurons in cell culture[13] and in animal models.[14] Increased Aβ42/Aβ40 ratios are commonly observed in familial Alzheimer's disease (FAD),[15,16] a rare form of AD caused by genetic mutations in proteins involved in Aβ production and characterized by earlier onset of dementia. FAD mutations within Aβ are often associated with faster aggregation and distinct aggregate morphology.[17] The Arctic FAD mutation E22G causes dementia at 55–60 years of age while sporadic AD usually affects people over 65. E22G aggregates into toxic protofibrils.[18] The Iowa FAD mutation D23N, causes dementia at 50–60 years of age and forms diffuse plaques.[19] Both Aβ mutants aggregates much faster than Aβ40.[17] In order to gain insight into the mechanism of altered aggregation, we carried out the first solution NMR studies of full length Aβ40–D23N and Aβ40–E22G monomers.

First, we characterized the backbone amide chemical shifts of Aβ40, Aβ42, Aβ40–D23N and Aβ40–E22G at ambient pressure. Recombinant ^{15}N-labeled peptides of all four Aβ species were produced with a protocol based on Glockshuber *et al.*[20] (see ESI†). Aβ42, Aβ40–D23N and Aβ40–E22G mostly cause localized change at the site of sequence variation (Fig. 1). Comparing Aβ42 with Aβ40, Fig. 1A illustrates that the addition of the two residues at the C-terminus mostly perturbed residue G37–V40. E22G also caused local changes, however the magnitude is extraordinary with a combined chemical shift perturbation (CSP) of ~15.7 ppm

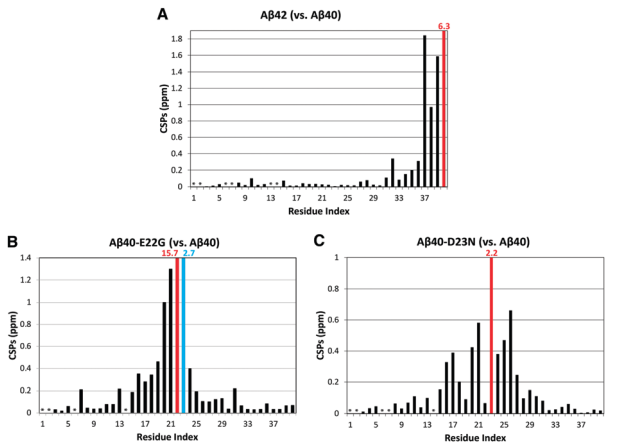

Fig. 1 Localized chemical shift perturbation (CSP) caused by Aβ42, as well as E22G and D23N FAD mutations compared with Aβ40. Combined ^{15}N and ^{1}H CSPs ($\mathrm{CSP} = \sqrt[2]{(10\Delta\delta_{\mathrm{H}})^2+(\Delta\delta_{\mathrm{N}})^2}$) are displayed here, with large CSP values outside the *y*-axis range represented by colored bars (red: mutation site; blue: D23 in E22G) with CSP values on top. Asterisks (*) were placed over residues which were unassigned in at least one of the spectra being compared, due to solvent/chemical exchange or spectral overlap.

[a] *Department of Biological Sciences, Rensselaer Polytechnic Institute, 110 Eighth Street, Troy, New York 12180, USA. E-mail: wangc5@rpi.edu*
[b] *Biochemistry and Biophysics Graduate Program, RPI, USA*
[c] *College of Arts and Sciences, Cornell University, Ithaca, NY14853, USA*
[d] *Center for Non Linear Studies, Los Alamos National Laboratory, Los Alamos, New Mexico 87545, USA*

† Electronic supplementary information (ESI) available. See DOI: 10.1039/c8cc01674g

($\Delta\delta_N$ = −13.16 ppm and $\Delta\delta_H$ = −0.86 ppm) at residue 22, with adjacent residues A21 and D23 also experiencing large shifts. We speculate that the large decrease of E22G amide proton shift (−0.86 ppm; see Fig. S2, panel for E22G, ESI†) is due to local conformational changes that brings F19 or F20 closer to G22, leading to a ring current effect.[21] Aβ40–D23N is a more conservative mutation, in contrast, with only residue 23 at the site of the mutation having a large perturbation.

To gain further insight into the structural mechanism of these Aβ variants, we carried out high pressure NMR. Pressure generally denatures proteins by favoring states that occupy lower volumes.[22] High pressure NMR spectroscopy has previously found extensive utility in the study of globular proteins,[22–29] including measurement of thermodynamic parameters, volume changes, and structural data about the intermediates of folding. Pressure also changes the residual structure and shifts population distribution of the partially structured ensembles of intrinsically disordered proteins (IDPs),[30,31] and the resulting perturbation in NMR spectra can allow us to identify residual structure and interactions in Aβ monomer ensemble. Among the four species of Aβ studied here, only high pressure NMR of Aβ40 has been carried out before.[30]

^1H–^{15}N HSQC spectra were collected ranging from ambient pressure to 2500 bar at 250 bar increments (Fig. 2 and Fig. S2, ESI†). For Aβ40, changes in peak position with pressure in overlaid HSQCs are nearly identical to those in previous work.[30] The pressure effect of chemical shift positions were analyzed by nitrogen and proton pressure coefficients from fitting chemical shift changes to a second order Taylor expansion with respect to pressure changes, after removing pressure effects observed in random coil model peptides[32] (see ESI†). As most peaks move in a straight line with pressure, the linear or first order B_1 pressure coefficient capture most of the pressure effect.

In Fig. 3, the nitrogen B_1 of three Aβ variants are compared with Aβ40. Overall, the B_1 profile over Aβ sequence is similar among all four Aβ species, characterized by marked elevated B_1 region between residue 11 and 21, and two flanking low B_1 regions, while the B_1 values near the C-terminus showed more variation. In contrast to localized changes at the site of mutation observed in CSP, a striking feature here is that L17 has the largest nitrogen B_1 increase in all three Aβ variants compared with slower aggregating Aβ40. L17 is part of CHC (LFVVA), which plays a crucial role in the mechanism of Aβ aggregation.[33] In addition, Q15 and K16, immediate N-terminal neighbors of L17, also have increased nitrogen B_1 in Aβ42, Aβ40–D23N and Aβ40–E22G.

To better understand implication of these changes in B_1, we investigated the correlation between B_1 and β-sheet propensity by comparing B_1 values and the percentage of β-population for each residue in replica exchange molecular dynamics (REMD) simulations of Aβ40 that we previously carried out using OPLS-AA and Amber99sb-ILDN force fields.[34] In general, despite it being a simplified representation of the ensemble, we can successfully use the overall ensemble β sheet content of Aβ40 in REMD simulations to explain much of the variation in the magnitude B_1 coefficients (Fig. 4). The β sheet profile agrees very well between simulations with the two different force fields, and that a quantitative comparison of these data with pressure coefficients, results in substantial PCCs of 0.5–0.6 for both force fields and for both nitrogen and hydrogen NMR data. It is remarkable that such a minimalist interpretation of the Aβ ensemble as the ensemble population of β sheet content per residue alone could capture so much of the variation seen in these NMR data.

Based on the correlation between B_1 and β-propensity, our data in Fig. 3 indicate that there is an increased β-propensity in the region Q15–L17 for the three fast-aggregating Aβ species examined here. This region overlaps with the CHC which is a key determinant of Aβ aggregation[33] and closely associated with plaque competence.[35] In addition, both NMR chemical shifts[36] and MD simulation[34,37,38] characterized CHC as having

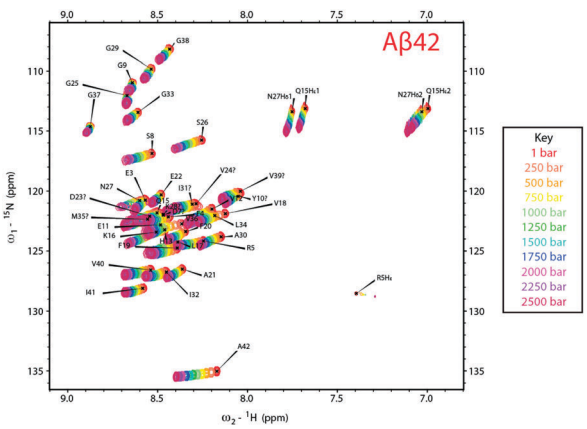

Fig. 2 High pressure NMR of monomer Aβ42. ^1H–^{15}N HSQC spectra for Aβ42 were collected with high pressure NMR, ranging from ambient pressure to 2500 bar at 250 bar increments. Assignments are shown on the spectra marked at their locations at 1 bar. Data were collected on a 600 MHz spectrometer at 277 K, using the high pressure pump and buffer conditions as described in the Methods in ESI.† High pressure NMR data for Aβ40, Aβ40–E22G and Aβ40–D23N are shown in Fig. S2 (ESI†).

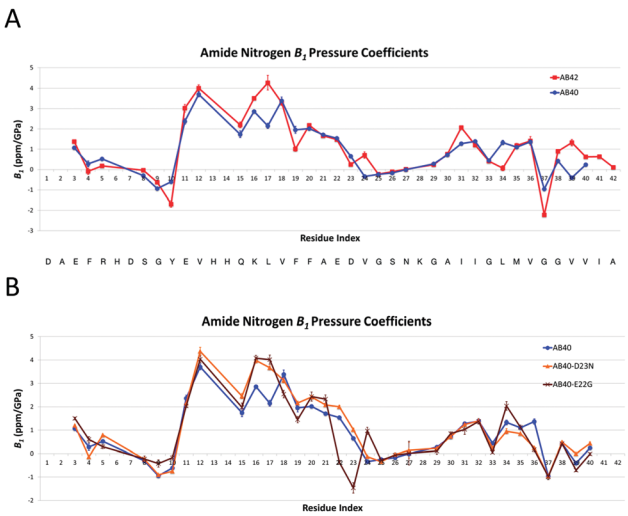

Fig. 3 Plot of the first order (B_1) pressure coefficients for the amide nitrogen nuclei. The sequence of wild type Aβ42 is presented in between the two graphs. B_2 coefficients of the second order Taylor polynomial are presented in Fig. S4 (ESI†).

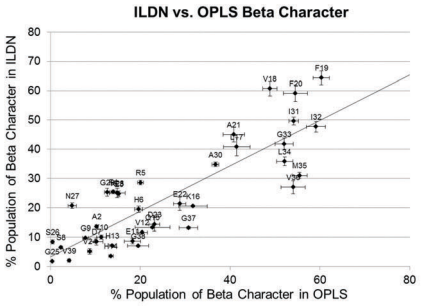

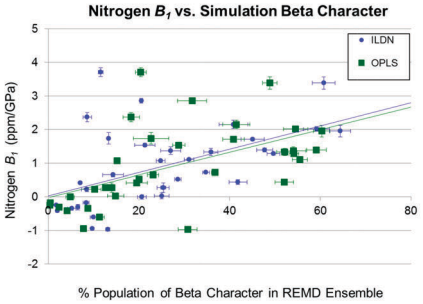

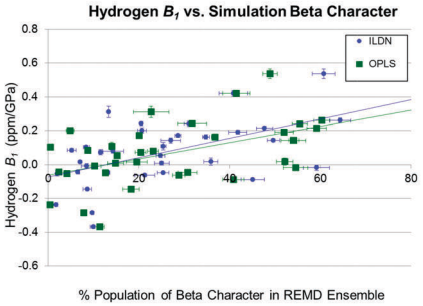

Pearson Correlation Coefficient (PCC)		
	OPLS β	ILDN β
OPLS β	1.00	0.85
Nitrogen B_1	0.55	0.52
Hydrogen B_1	0.50	0.54

Fig. 4 Correlation analysis for Aβ40 relating β sheet character annotated through REMD simulations using DSSP with first order (B_1) pressure coefficients. "OPLS" and "ILDN" here denote Aβ simulation carried out previously with replica exchange molecular dynamics (REMD) simulations of Aβ conducted with two different force fields, OPLS-AA/TIP3P and AMBER99sb-ILDN/TIP4P-Ew combinations, respectively (see ESI†).[34,38]

the highest β-propensity in Aβ sequences. Thus Aβ42, D23N and E22G may all stabilize the β-conformation at CHC and/or extend the β-strand further towards the N-terminus, which likely enhances aggregation rate and seed formation.

Besides the B_1 increase near the CHC region, we also note other changes in B_1 that are not present in CSP. Aβ40–E22G specifically produces distinctive changes in the pattern of pressure coefficients (Fig. 3B). E22G dramatically reduces D23 nitrogen B_1 (Fig. 3B) to be negative, while G22 has nitrogen B_1 close to zero. A reduction in nitrogen B_1 indicates a decreased β-population in this area. Combined with increased B_1 at

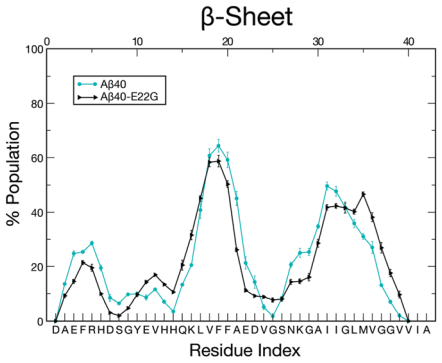

Fig. 5 Comparison of % β-sheet of wild type Aβ40 and Aβ40–E22G in AMBER99sb-ILDN REMD simulations, showing a positional shift of CHC β population towards to N-terminus in the mutant ensemble. Adapted from Rosenman *et al.*[34]

Q15–L17, high pressure NMR data suggests a positional shift of β-population towards the N-terminus caused by the E22G mutation. In REMD simulations of Aβ40–E22G,[34] this positional shift has indeed been observed, with increased β-content at Q15, K16 and L17 and decreased β-content at E22 (Fig. 5). Thus the E22G FAD mutation causes a unique conformational bias in Aβ monomer, which likely contributes to its unique propensity to form protofibrils.

Fig. 3A also reveals significant changes in pressure coefficients between the Aβ40 and Aβ42 forms at the C-terminus. Residue 38–40 have significantly elevated B_1 in Aβ42 compared with Aβ40. One model consistent with the observed trends in pressure coefficient of Aβ42 *versus* Aβ40 is the sampling of a new C-terminal β hairpin with a turn at G37 (characterized by low B_1), which is observed through REMD simulations[34,38] of Aβ42 monomer, and in oligomer[39–42] and fibril[43–45] structures of Aβ42.

In summary, high pressure NMR measurements provide new insights into the conformational perturbation caused by FAD mutations in Aβ, a crucial molecule in AD pathogenesis. All three fast aggregating species Aβ42, E22G and D23N have increased pressure sensitivity at residue Q15–L17, indicating an increased β-propensity for CHC. High pressure NMR also indicates that E22G causes a shift in CHC β-population, corroborated by REMD. Further, changes in Aβ42's pressure coefficients at the C-terminus is consistent with the sampling a C-terminal β-hairpin not present in Aβ40. Overall, high pressure NMR characterization of Aβ here is consistent with the β hairpin dominated ensembles observed through REMD simulations with two different force fields.[34,38] We have established previously[34,38] that β hairpin conformations seen in Aβ monomer simulations bear structural similarity to intrapeptide models of higher order aggregates such as oligomers and fibrils based on solid state NMR data.[39,46–48] The high pressure NMR data here support the idea that free Aβ monomers can indeed sample these hairpin conformations, and that these could act as seeds of aggregation. Subtle changes in the ensemble as suggested by these data, such as an additional C-terminal turn in Aβ42 and shifting of β-population at CHC in Aβ40–E22G, could seed of new pathways that enhance aggregation and results in unique aggregation properties.

This study also demonstrates that high pressure NMR is a powerful tool for revealing subtle conformational biases in intrinsically disordered proteins.

We thank Dr. Catherine Royer and Martin Fossat for access and help with high pressure NMR equipment.

Conflicts of interest

There are no conflicts to declare.

Notes and references

1 M. Prince, A. Wimo, M. Guerchat, G.-C. Ali, Y.-T. Wu and M. Prina, *Alzheimer's Dis. Int. World Alzheimer Rep.*, 2015, 1–84.
2 J. T. Jarrett, E. P. Berger and P. T. Lansbury, *Biochemistry*, 1993, **32**, 4693–4697.
3 Y. Yan and C. Wang, *J. Mol. Biol.*, 2006, **364**, 853–862.
4 G. Bitan, M. D. Kirkitadze, A. Lomakin, S. S. Vollers, G. B. Benedek and D. B. Teplow, *Proc. Natl. Acad. Sci. U. S. A.*, 2003, **100**, 330–335.
5 C. L. Masters, R. Cappai, K. J. Barnham and V. L. Villemagne, *J. Neurochem.*, 2006, **97**, 1700–1725.
6 T. Luhrs, C. Ritter, M. Adrian, D. Riek-Loher, B. Bohrmann, H. Dobeli, D. Schubert and R. Riek, *Proc. Natl. Acad. Sci. U. S. A.*, 2005, **102**, 17342–17347.
7 A. Lorenzo and B. A. Yankner, *Proc. Natl. Acad. Sci. U. S. A.*, 1994, **91**, 12243–12247.
8 J. D. Harper, S. S. Wong, C. M. Lieber and P. T. Lansbury, *Chem. Biol.*, 1997, **4**, 119–125.
9 I. Benilova, E. Karran and B. De Strooper, *Nat. Neurosci.*, 2012, **15**, 349–357.
10 B. J. Cummings and C. W. Cotman, *Lancet*, 1995, **346**, 1524–1528.
11 Y. M. Kuo, M. R. Emmerling, C. Vigo-Pelfrey, T. C. Kasunic, J. B. Kirkpatrick, G. H. Murdoch, M. J. Ball and A. E. Roher, *J. Biol. Chem.*, 1996, **271**, 4077–4081.
12 C. A. McLean, R. A. Cherny, F. W. Fraser, S. J. Fuller, M. J. Smith, K. Beyreuther, A. I. Bush and C. L. Masters, *Ann. Neurol.*, 1999, **46**, 860–866.
13 O. M. El-Agnaf, D. S. Mahil, B. P. Patel and B. M. Austen, *Biochem. Biophys. Res. Commun.*, 2000, **273**, 1003–1007.
14 L. Mucke, E. Masliah, G. Q. Yu, M. Mallory, E. M. Rockenstein, G. Tatsuno, K. Hu, D. Kholodenko, K. Johnson-Wood and L. McConlogue, *J. Neurosci.*, 2000, **20**, 4050–4058.
15 N. Suzuki, T. T. Cheung, X. D. Cai, A. Odaka, L. Otvos, C. Eckman, T. E. Golde and S. G. Younkin, *Science*, 1994, **264**, 1336–1340.
16 M. Citron, T. Oltersdorf, C. Haass, L. McConlogue, A. Y. Hung, P. Seubert, C. Vigo-Pelfrey, I. Lieberburg and D. J. Selkoe, *Nature*, 1992, **360**, 672–674.
17 A. Hatami, S. Monjazeb, S. Milton and C. G. Glabe, *J. Biol. Chem.*, 2017, **292**, 3172–3185.
18 C. Nilsberth, A. Westlind-Danielsson, C. B. Eckman, M. M. Condron, K. Axelman, C. Forsell, C. Stenh, J. Luthman, D. B. Teplow, S. G. Younkin, J. Näslund and L. Lannfelt, *Nat. Neurosci.*, 2001, **4**, 887–893.
19 T. A. Neubert, Y. Lu, G. W. Rebeck, B. Frangione, S. M. Greenberg and J. Ghiso, *Am. J. Pathol.*, 2010, **176**, 1841–1854.
20 V. H. Finder, I. Vodopivec, R. M. Nitsch and R. Glockshuber, *J. Mol. Biol.*, 2010, **396**, 9–18.
21 S. J. Perkins and K. Wüthrich, *Biochim. Biophys. Acta, Protein Struct. Mol. Enzymol.*, 1979, **576**, 409–423.
22 C. A. Royer, *Biochim. Biophys. Acta, Protein Struct. Mol. Enzymol.*, 2002, **1595**, 201–209.
23 K. Inoue, H. Yamada, K. Akasaka, C. Herrmann, W. Kremer, T. Maurer, R. Doker and H. R. Kalbitzer, *Nat. Struct. Biol.*, 2000, **7**, 547–550.
24 M. W. Lassalle, H. Yamada and K. Akasaka, *J. Mol. Biol.*, 2000, **298**, 293–302.
25 K. Kuwata, H. Li, H. Yamada, C. A. Batt, Y. Goto and K. Akasaka, *J. Mol. Biol.*, 2001, **305**, 1073–1083.
26 R. Kitahara, S. Yokoyama and K. Akasaka, *J. Mol. Biol.*, 2005, **347**, 277–285.
27 M. W. Lassalle and K. Akasaka, in *Protein Folding Protocols*, ed. Y. Bai and R. Nussinov, Humana Press, Totowa, NJ, 2006, vol. 350, pp. 21–38.
28 R. Kitahara, K. Hata, H. Li, M. P. Williamson and K. Akasaka, *Prog. Nucl. Magn. Reson. Spectrosc.*, 2013, **71**, 35–58.
29 A. S. Zwarycz, M. Fossat, O. Akanyeti, Z. Lin, D. J. Rosenman, A. E. Garcia, C. A. Royer, K. V. Mills and C. Wang, *Biochemistry*, 2017, **56**, 2715–2722.
30 C. E. Munte, M. Beck-Erlach, W. Kremer, J. Koehler and H. R. Kalbitzer, *Angew. Chem., Int. Ed.*, 2013, **52**, 8943–8947.
31 J. Roche, J. Ying, A. S. Maltsev and A. Bax, *ChemBioChem*, 2013, **14**, 1754–1761.
32 J. Koehler, M. Beck Erlach, E. Crusca, W. Kremer, C. E. Munte and H. R. Kalbitzer, *Materials*, 2012, **5**, 1774–1786.
33 N. S. De Groot, F. X. Aviles, J. Vendrell and S. Ventura, *FEBS J.*, 2006, **273**, 658–668.
34 D. J. Rosenman, C. Wang and A. E. García, *J. Phys. Chem. B*, 2016, **120**, 259–277.
35 W. P. Esler, E. R. Stimson, J. R. Ghilardi, Y. A. Lu, A. M. Felix, H. V. Vinters, P. W. Mantyh, J. P. Lee and J. E. Maggio, *Biochemistry*, 1996, **35**, 13914–13921.
36 L. Hou, H. Shao, Y. Zhang, H. Li, N. K. Menon, E. B. Neuhaus, J. M. Brewer, I. J. L. Byeon, D. G. Ray, M. P. Vitek, T. Iwashita, R. a. Makula, A. B. Przybyla and M. G. Zagorski, *J. Am. Chem. Soc.*, 2004, **126**, 1992–2005.
37 N. G. Sgourakis, Y. Yan, S. A. McCallum, C. Wang and A. E. Garcia, *J. Mol. Biol.*, 2007, **368**, 1448–1457.
38 D. J. Rosenman, C. R. Connors, W. Chen, C. Wang and A. E. García, *J. Mol. Biol.*, 2013, **425**, 3338–3359.
39 M. Ahmed, J. Davis, D. Aucoin, T. Sato, S. Ahuja, S. Aimoto, J. I. Elliott, W. E. Van Nostrand and S. O. Smith, *Nat. Struct. Mol. Biol.*, 2010, **17**, 561–567.
40 C. Lendel, M. Bjerring, A. Dubnovitsky, R. T. Kelly, A. Filippov, O. N. Antzutkin, N. C. Nielsen and T. Härd, *Angew. Chem., Int. Ed.*, 2014, **53**, 12756–12760.
41 B. Strodel, J. W. L. Lee, C. S. Whittleston and D. J. Wales, *J. Am. Chem. Soc.*, 2010, **132**, 13300–13312.
42 L. Nagel-steger, M. C. Owen and B. Strodel, *ChemBioChem*, 2016, 657–676.
43 Y. Xiao, B. Ma, D. McElheny, S. Parthasarathy, F. Long, M. Hoshi, R. Nussinov and Y. Ishii, *Nat. Struct. Mol. Biol.*, 2015, **22**, 499–505.
44 M. A. Wälti, F. Ravotti, H. Arai, C. G. Glabe, J. S. Wall, A. Böckmann, P. Güntert, B. H. Meier and R. Riek, *Proc. Natl. Acad. Sci. U. S. A.*, 2016, 201600749.
45 M. T. Colvin, R. Silvers, Q. Z. Ni, T. V. Can, I. Sergeyev, M. Rosay, K. J. Donovan, B. Michael, J. Wall, S. Linse and R. G. Griffin, *J. Am. Chem. Soc.*, 2016, **138**, 9663–9674.
46 A. T. Petkova, W. M. Yau and R. Tycko, *Biochemistry*, 2006, **45**, 498–512.
47 A. K. Paravastu, R. D. Leapman, W. M. Yau and R. Tycko, *Proc. Natl. Acad. Sci. U. S. A.*, 2008, **105**, 18349–18354.
48 I. Bertini, L. Gonnelli, C. Luchinat, J. Mao and A. Nesi, *J. Am. Chem. Soc.*, 2011, **133**, 16013–16022.

